Journal of Integrative Agriculture 2026, 25(3): 1263–1275

Available online at ScienceDirect

Journal of Integrative Agriculture



RESEARCH ARTICLE

Microplastics reduce the wheat (*Triticum aestivum* L.) net photosynthetic rate through rhizospheric effects

Yuhuai Liu[1, 2, 3, 4], Heng Wang[4], Li Wang[2], Jina Ding[2], Hui Zhai[4], Qiujin Ma[3, 4], Can Hu[5], Tida Ge[1, 2#]

[1] *College of Smart Agriculture, Xinjiang University, Urumqi 830017, China*
[2] *State Key Laboratory for Quality and Safety of Agro-Products, International Science and Technology Cooperation Base for the Regulation of Soil Biological Functions and One Health of Zhejiang Province, Ningbo University, Ningbo 315211, China*
[3] *Ecological Postdoctoral Research Station, Xinjiang University, Urumqi 830046, China*
[4] *College of Ecology and Environment, Xinjiang University, Urumqi 830017, China*
[5] *College of Mechanical and Electrical Engineering, Tarim University, Alar 843300, China*

Highlights

- Microplastics decrease superoxide dismutase but increase peroxidase activities.
- Microplastics decrease bacterial and fungal diversity indices in rhizosphere soil.
- Microplastics decrease bacterial network complexity in rhizosphere soil.
- Microplastics increase fungal network complexity in rhizosphere soil.
- Microplastic-induced changes in antioxidant enzymes reduce the net photosynthetic rate.

Abstract

Microplastic accumulation after film mulching affects nutrients cycling in the soil–crop system. Bulk soil (BS) and rhizosphere soil (RS) have two different community compositions which lead to their different microbial nutrient acquisition abilities. Microplastics influence the rhizosphere effect. However, the mechanism by which microplastic accumulation affects the net photosynthetic rate (NPR) through rhizospheric microbial communities remains unknown. This study aimed to identify the mechanisms underlying the effects of polyethylene (PE) and polyvinyl chloride (PVC) microplastics at 0, 1, and 5% (w/w) on the NPR in the wheat–soil ecosystem using a pot experiment. Superoxide dismutase (SOD) activity was reduced by 15.35–36.7%, and that of peroxidase (POD) was increased by 32.47–61.93%, causing reductions in NPR (17.94–23.81%) in the PE5% and PVC (1 and 5%) (w/w) treatments compared with the control. The Chao1, Shannon, and Simpson indices of the bacterial and fungal diversities were lower in BS than in RS at PE1% and PVC5% (w/w), respectively. The bacterial and fungal network complexities were reduced and increased, respectively, owing to alterations in the bacterial and fungal community compositions and structures for wheat growth. The Mantel test showed that the bacterial and fungal diversity indices in BS had positive correlations with Olsen-P and phosphatase; however, those in RS were positively correlated with NO_3^- and β-1,4-glucosidase. The structural equation model indicated that wheat enzymatic and soil hydrolytic activities negatively affected NPR. Wheat has a profound antioxidant defense strategy for PE and PVC microplastic stress, which produces a synergistic effect of POD by protecting organelles and reducing tissue damage to preserve the NPR.

Keywords: microplastics, microbial community, hydrolases, bacteria and fungi, wheat

1. Introduction

Plastic mulch films are used worldwide in agricultural practices because their application enhances crop yields (Ng *et al*. 2018; Liu *et al*. 2023). However, microplastic accumulation (particles<5 mm in size) after agricultural film mulching significantly alters the crop–soil system, and affects the high-quality development of agricultural practices (Brodhagen *et al.* 2017; Song *et al.* 2024). The two primary

Received 24 January 2025; Received in revised form 2 April 2025; Accepted 19 May 2025; Available online 9 June 2025
#Correspondence Tida Ge, E-mail: getida@nbu.edu.cn

© 2026 CAAS. Publishing services by Elsevier B.V. on behalf of KeAi Communications Co. Ltd. This is an open access article under the CC BY-NC-ND license (http://creativecommons.org/licenses/by-nc-nd/4.0/). Peer review under responsibility of Editorial Board of *Journal of Integrative Agriculture*.
doi: 10.1016/j.jia.2025.06.014

types of microplastics currently used in agriculture are polyethylene (PE) and polyvinyl chloride (PVC) because of their low cost (Zhou *et al.* 2021; Liu Y *et al.* 2022). PE is a highly crystalline complex molecular substance with varying molecular weights and weight distributions (Aggarwal and Sweeting 1957). PVC reportedly loses hydrogen chloride and becomes colored when exposed to heat or light, and the polymer becomes stiff and insoluble because of crosslinking (Winkler 1959). Therefore, PVC has been prohibited in agricultural practices, including in China; however, its residual effects remain significant (Liu Y *et al.* 2022).

Microplastic accumulation alters the soil structure, reduces soil bulk density, and improves saturated hydraulic conductivity, and the attachment of microorganisms to the microplastic surface is facilitated by increases in the attachment sites (De Tender *et al.* 2017; de Souza Machado *et al*. 2018), through the formation of oligomers, dimers, and monomers during biodegradation (Ganesh Kumar *et al.* 2020). Microplastics disrupt soil nutrient cycling (carbon (C), nitrogen (N), and phosphorus (P)) by affecting the secretion of microbial C-, N-, and P-related hydrolases and the microbiome, as well as ecosystem multifunctionality (Lozano *et al.* 2021; Sun *et al.* 2022; Yin *et al.* 2023), which are highly correlated with the type and dose of microplastics (Zang *et al.* 2020; Sun *et al*. 2022). For example, PE microplastics reduce dissolved organic C (DOC), nitrate-N (NO_3^-), and Olsen-P concentrations by inhibiting the activities of C- (β-1,4-glucosides) and N- (protease or urease) related hydrolases or increasing the P- (alkaline phosphatase) related hydrolases, thereby promoting soil organic matter (SOM) decomposition due to the increased turnover rate of soil bacterial communities and the bacterial community-induced intensification of SOM consumption (Xiao *et al.* 2022; Liu *et al.* 2024). However, the degree of soil crystallinity is promoted by PVC microplastic input, which reduces the adsorption capacities of the soil and affects microbial activities and soil structure (Khan *et al.* 2021). PVC microplastics reduce the soil NO_3^- concentration by increasing the soil denitrification potential and altering the soil bacterial community, which stimulates SOM decomposition (Ma *et al.* 2024). In crop–soil ecosystems, bulk soil (BS) and rhizosphere soil (RS) have varying microbial nutrient acquisition potentials and community composition sites because root exudates are a constant source of soluble C resource input to the soil during crop growth (Liu *et al.* 2021). PE and PVC microplastics at 0.01% and 1% (w/w) alter the below-ground partitioning of crop photosynthetic and rhizodeposited C utilization through the microbiota, and they increase arbuscular mycorrhizal fungi and Zygomycota by 175 and 197%, respectively, which then drive photosynthetic and rhizodeposited C incorporation into the SOM (Hu *et al.* 2024). In our previous study, compared with the effects of low doses (1% (w/w)) of PE and PVC microplastics, PE5% (w/w) microplastics caused the rapid consumption of rhizospheric NH_4^+ and NO_3^-; however, PVC5% (w/w) microplastics forced the roots to obtain available nutrients in a narrow root zone, causing the roots to release abundant labile C to stimulate microbial metabolism and N mining (Liu S *et al.* 2022). Regarding crop enzymes, PE microplastics increase superoxide dismutase (SOD) activity but do not alter peroxidase (POD) activity (Zhang *et al*. 2022). In contrast, PVC microplastics increase both SOD and POD activities (Zhang *et al.* 2024), which negatively influence the net photosynthetic rate (NPR) of crops (Ren *et al.* 2021; Hu *et al.* 2024). Nevertheless, how the differences in BS and RS microbial communities affect the NPR for crop growth through the rhizospheric effects under PE and PVC microplastic accumulation remains unknown.

This study explored how PE and PVC microplastics affect the microbial communities in BS and RS and further influence the NPR through microbial and crop root nutrient acquisition strategies during crop growth. We hypothesized that: (1) low-dose PE microplastics increase NO_3^- with N hydrolase hotspots and the rhizospheric expansion of P hydrolase by increasing bacterial diversity; (2) high-dose PVC microplastics increase the hotspots and rhizospheric expansion of C hydrolase but reduce that of P hydrolases by increasing fungal diversity; and (3) PE and PVC microplastics reduce the SOD activity but increase the POD activity through rhizospheric effects, thus affecting the NPR. To test these hypotheses, *in situ* soil zymography techniques were used with available nutrients (DOC, NH_4^+, NO_3^-, and Olsen-P), related hydrolases (β-1,4-glucosidase (BG), β-1,4-xylosidase (XYL), 4-N-acetyl-glucosaminidase (NAG), and phosphatase PHOS), and bacterial and fungal community diversities (Chao1, Shannon, and Simpson indices) and compositions to elucidate how PE and PVC microplastics affect the NPR through SOD and POD activities.

2. Materials and methods

2.1. Soil sampling

In March 2021, the topsoil samples (0–20 cm) in this study were manually collected from the plow layer in a wheat field located in Linyi City, Shandong Province, China (35°6.57′N, 118°38.14′E). This area has a warm, sub-humid continental climate with a mean annual temperature and precipitation of 14.1°C and 886 mm, respectively. The soil is aquic brown. After collection, the soil samples were sieved (<5 mm) under field-moist conditions to manually homogenize them and remove fine roots and other plant or animal residues. The soil physicochemical properties were pH, 5.16; organic C, 24.60 g kg^{-1}; total N, 3.19 g kg^{-1}; NO_3^-, 59.33 mg kg^{-1}; and NH_4^+, 40.30 mg kg^{-1} (Liu Y *et al.* 2022).

2.2. Experimental design and setup

The soils were supplemented with based fertilizer at 750 kg ha^{-1} (nitrogen:phosphorus pentoxide:potassium oxide ($N:P_2O_5:K_2O$)=14:7:9) and pre-incubated at 25°C for 2 weeks before starting the experiment. Two common microplastics, PE and PVC microplastics (125 μm; Sigma-Aldrich, St. Louis, USA), were used in this study. The addition gradient was set at 0%, 1% (10,000 mg (w/w) kg^{-1} dry soil), and 5% (50,000 mg (w/w) kg^{-1} dry soil) (Liu Y *et al.* 2022). Therefore, the experiment included five treatments: (i) no PE or PVC microplastic addition (CK), (ii) 1% PE microplastic addition (PE1% (w/w)), (iii) 5% PE microplastic addition (PE5% (w/w)), (iv) 1% PVC microplastic addition (PVC1%, w/w), and (v) 5%

PVC microplastic addition (PVC5%, w/w), and each treatment had three replicates. Wet soil (approximately 0.7 kg dry) was evenly packed into a rhizobox (20.5 cm×13.4 cm×5.2 cm) with one removable side after the soils were pre-treated. Then, wheat (*Triticum aestivum* L.) seeds were germinated, and the seedlings were transplanted into the center of the applicable rhizobox and watered every three days. The soil moisture was maintained at a gravimetric moisture content of 20% during the experiment. Next, the rhizoboxes were inclined at 60° to ensure that the root system adhered to the glass wall, facilitating the distinction between the RS and BS. All treatments were kept in a glasshouse under a day/night temperature regime of (25±1/20±1)°C for 60 days.

2.3. Zymography image analysis

The soil zymography image analysis was performed by applying polyamide membranes (155 cm×115 cm, 0.45 μm; Taoyuan Med-Chem Instrument Co., Ltd., China) saturated with 4-methylmbelliferone (MUF)-labeled substrates (BG, XYL, NAG, and PHOS) to the soil surface at 60 days after planting in a rhizobox with transparent glass (Wei *et al.* 2019; Bilyera *et al.* 2020; Liu Y *et al.* 2022). Briefly, BG, XYL, NAG, and PHOS were dissolved in sodium morpholine-4-ethanesulfonate ($C_6H_{13}NO_4SNa_{0.5}$) buffer at 10 mmol L^{-1}. The zymographic membranes for each hydrolase were tightly adhered to the surface of the root–soil in the rhizobox, incubated for 2 h in the dark at the ambient indoor temperature, and carefully lifted off the surface of the root-soil. Then, a zymographic image of each membrane was taken with a high-definition camera (D7000, Nikon, Japan) under ultraviolet (UV) illumination at an extraction wavelength of 355 nm. The spatial distribution of the activity of each hydrolase was quantified using Fiji software (version 1.8, National Institutes of Health, Wayne Rasband, USA). Next, the activities of the four hydrolases were converted to 8-byte grayscale values for calculating the mean and standard deviation (SD) according to a standard MUF curve of 0.01, 0.2, 0.5, 1, 2, 4, 6, and 10 mmol L^{-1}. Hydrolase activity intensities greater than the mean+3SD were considered hotspots (Bilyera *et al.* 2020). The results are presented as a percentage of the total soil surface area (Liu Y *et al.* 2022). Individual root systems were used as references to draw a perpendicular line to the root. Finally, the inter-rhizosphere value was obtained by converting the horizontal units to millimeters according to the number of pixels and the image resolution (Liu Y *et al.* 2022).

2.4. Enzymes and NPR of wheat

The activities of SOD and POD in wheat were assessed using the nitrogen blue tetrazolium and guaiacol methods, respectively (Jebara *et al.* 2005; Zhang and Li 2005). For SOD activity, wheat leaves were collected and the veins were removed. Leaf samples (0.5 g) were weighed in a pre-cooled mortar, to which 2 mL of pre-cooled phosphate buffer (pH 7.8) was added, followed by grinding to a homogenate on an ice bath and the addition of phosphate buffer to yield a final volume of 5 mL. The supernatant was extracted, and its absorbance was measured at 560 nm using a UV-visible (Vis) spectrophotometer (UV-2450, Shimadzu Corporation, Japan). For POD activity, a 1 g plant leaf sample was weighed, sectioned into pieces, and placed into a mortar that had been frozen. A small amount of quartz sand was added, followed by adding 10 mL of phosphate buffer (pH 7.0) twice, grinding into a homogenate, and centrifugation in a centrifuge tube. The resulting supernatant was the crude enzyme extract. Approximately 80 mL of 0.1 mol L^{-1} phosphate buffer (pH 7.0) and 0.5 mL of guaiacol were added to the extracted supernatant and shaken vertically to fully dissolve the guaiacol, and 1 mL of 30% H_2O_2 was added. The supernatant was extracted, and its absorbance was measured at 470 nm using a UV-Vis spectrophotometer (UV-2450, Shimadzu, Japan). The NPR was assessed using an Li-6400 photosynthesis system (version 4, LI-COR, USA).

2.5. Sampling and physicochemical properties of soil

The wheat samples, RS and BS, were collected after the zymography image analysis and stored at 4°C for further analyses. The 0.5 mol L^{-1} K_2SO_4 extracts of the samples were analyzed using a multi N/C 2100 TOC/TN analyzer (Analytik Jena, Jena, Germany) to measure soil DOC and an auto-analyzer (AA3, SEAL, Germany) to determine the NH_4^+ and NO_3^- concentrations (Liu *et al.* 2020). Olsen-P was determined using a 0.5 mol L^{-1} $NaHCO_3$ extract (1:20 w/v, pH=8.5) and a UV-Vis spectrophotometer (UV-2450, Shimadzu, Japan) (Olsen *et al.* 1954).

The potential activities of soil extracellular hydrolases, including BG, XYL, NAG, and PHOS, were evaluated based on a modified version of the methods used in previous studies (Terefe *et al.* 2010; Liu *et al.* 2020). The activities of the four hydrolases were determined fluorometrically (excitation at 365 nm, emission at 450 nm) using a substrate linked to a fluorescent tag (a 50 μL aliquot of 100 μmol L^{-1} MUF in each sample well) (Yuan *et al.* 2017). The hydrolase activities were quantified using an automated fluorometric plate reader (Victor3 1420–050 Multi-label Counter; PerkinElmer, Waltham, MA, USA).

2.6. Bacterial and fungal communities

Total genomic DNA was extracted from 0.5 g of frozen soil (–80°C) using the DNeasy PowerSoil Kit (Qiagen, Hilden, Germany). The DNA concentration and quality were measured using a Nanodrop spectrophotometer (ND-100; Thermo Fisher Scientific, Waltham, MA, USA). The universal forward primer 341 F and reverse primer 806 R were used to amplify the bacterial hypervariable V3–V4 regions of the 16S rRNA gene (Wei *et al.* 2020). The ITS region was targeted for fungi using the primers ITS1F and ITS2 (Liu *et al.* 2024). The PCR products were purified using a Qiagen Gel Extraction Kit (Qiagen, Germany) and sequenced on an Illumina MiSeq platform (Novogene Co., Ltd., Beijing, China). Following the manufacturer's instructions, sequencing libraries were generated using the NEBNext® Ultra™ II DNA Library Prep Kit for Illumina® (New England Biolabs, MA, USA). The index codes were added, and the library quality was assessed using the Qubit® 2.0 fluorometer (Thermo Fisher Scientific, MA, USA). Finally, the library was sequenced on an Illumina

platform, and 250 bp paired-end reads were generated. The raw sequences were processed using quantitative insights into microbial ecology (QIIME, version 1.7.0), following the online instructions (Caporaso *et al.* 2010). Sample-splitting was performed to determine the origin of each sequence. Sequence denoising was performed to obtain amplicon sequence variants (ASVs) and reduce sequencing errors and redundancy. After obtaining the feature list (ASV list) and representative sequences, species annotation was performed for bacteria, fungi, and protists. ASVs with total sequences of less than 20 were filtered out, and the resulting bacterial, fungal, and protist samples were individually flattened. The linear discriminant analysis (LDA) effect size was applied to identify the vital microbial taxa (phyla) that differed significantly between the BS and RS. In addition, individual subnetworks were constructed for BS and RS to facilitate a comparative analysis of their network topologies with the subgraph functions provided by the "igraph" package.

2.7. Statistical analyses

All figures and statistical analyses were generated using R software (version 4.0.0). Levene's test for homogeneity of variance was performed, and the means for each treatment (CK, PE1%, PE5%, PVC1%, and PVC5%) were compared using the "agricolae" package with a least significant difference of 5% ($LSD_{0.05}$). FastSpar (version 1.0.0), incorporating the SparCC algorithm, was used to infer microbial correlation networks. All data were divided into two parts (BS and RS) for all treatments, and the bacterial and fungal communities to determine the cooccurrence networks of their communities. Subsequently, the correlations and *P*-values among the ASVs were inferred using 50 iterations and 1,000 permutations. Significant ($P<0.05$) correlations with coefficients of >0.7 or <0.7 were used. The correlations were visualized, and their topological features were calculated using Gephi (version 0.9.2), including key network metrics (the number of nodes (N) and edges (E)), by running each treatment (control, PE1%, PE5%, PVC1%, and PVC5%) in the BS and RS together. Mantel analysis was performed using the "ggcor" and "linkET" packages in R to test the significance of relationships between soil chemical properties (DOC, NH_4^+, NO_3^-, Olsen-P, BG, XYL, NAG, and PHOS) and bacterial and fungal diversity indices (Chao1, Shannon, and Simpson) for BS and RS. Structural equation modeling (SEM) was performed using the "Lavaan" package in R to test the significance of the hypothesized causal relationships among the type and content of microplastics, microbial biomass, soil enzymatic activities, available nutrients, microbial diversity, and physiological growth of the plants. Before SEM analysis, the DOC, NH_4^+, NO_3^-, and Olsen-P were downgraded into available nutrients; SOD and POD were downgraded into plant enzymatic activity, the activities of BG, XYL, NAG, and PHOS were downgraded into soil enzyme activity, the bacterial Chao1, Shannon, and Simpson indices were downgraded into soil bacterial diversity, and the fungal Chao1, Shannon, and Simpson indices were downgraded into soil fungal diversity. The NPR was standardized. The best-fit model was determined using Chi-square, *P*-values, goodness-of-fit index (GFI), root-mean-square error of approximation (RMSEA), and standard root mean square residual (SRMR). Based on the removal and addition relationships between the observed variables, an optimal model was built, and the standardized estimate value (R^2) and standardized total effects, as well as the effect of microplastic addition on the NPR of wheat, were obtained.

3. Results

3.1. Plant enzymic activities and NPR

SOD activity significantly decreased by 15.35, 40.06, and 36.70% under the PE5%, PVC1%, and PVC5% (w/w) treatments, respectively, compared with CK (Fig. 1-A). However, POD activity significantly increased by 32.47, 66.22, and 61.93% in the PE5%, PVC1%, and PVC5% (w/w) treatments, respectively, compared with CK (Fig. 1-B). The NPR significantly decreased by 22.51, 23.81, and 17.94% in the PE5%, PVC1%, and PVC5% (w/w) treatments, respectively, compared with CK (Fig. 1-C).

3.2. Available soil nutrients

The soil DOC concentration was significantly higher in BS than

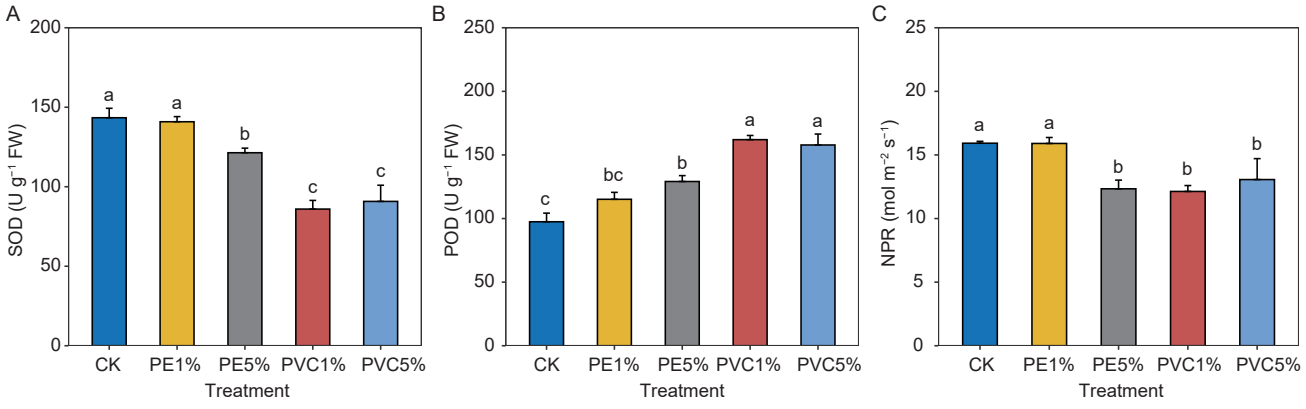


Fig. 1 Activities of superoxide dismutase (SOD; A) and peroxidase (POD; B) and net photosynthetic rate (NPR; C) in the soil under five treatments. Treatments include no polyethylene or polyvinyl chloride addition (CK), 1% polyethylene addition (PE1%, w/w), 5% polyethylene addition (PE5%, w/w), 1% polyvinyl chloride addition (PVC1%, w/w), and 5% polyvinyl chloride addition (PVC5%, w/w). Different lowercase letters indicate significant differences ($P<0.05$) among the five treatments. All results are mean±SE ($n=3$).

in RS under the PE5% and PVC (1 and 5%) (w/w) treatments. The DOC concentrations in BS and RS did not change (P>0.05) in the PE and PVC (1 and 5%) (w/w) treatments compared with CK (Fig. 2-A). The NH_4^+ concentration was significantly higher in BS than in RS under the CK, PE (1 and 5%), and PVC1% (w/w) treatments. The NH_4^+ concentration in BS was significantly higher in the PVC1% (w/w) treatment but significantly lower in the PVC5% (w/w) treatment compared to CK. The NH_4^+ concentration in RS did not change (P>0.05) in the PE and PVC (1 and 5%)(w/w)) treatments compared with CK (Fig. 2-B). The NO_3^- concentration was significantly higher in BS than in RS under CK and the treatments with PE (1 and 5%) and PVC1% (w/w). The NO_3^- concentration in BS was significantly lower in PVC5% (w/w) than in CK. The NO_3^- concentration in RS was significantly higher in the PE (1 and 5%) (w/w) treatment than in CK (Fig. 2-C). The Olsen-P concentration was significantly higher in BS than in RS under treatment with PE1% (w/w) but significantly lower in BS than in RS under the PVC5% (w/w) treatment. The Olsen-P concentration in BS was significantly higher under the PE1% (w/w) treatment than in CK; however, the concentration in RS did not change (P>0.05) under either PE or PVC (1 and 5%) treatment compared with the CK treatment (Fig. 2-D).

3.3. Soil potential hydrolytic activities

Soil BG activity was significantly higher in BS than in RS under treatments with CK and PE (1 and 5%) (w/w). Soil BG activity in BS was significantly higher in the PE5% and PVC5% (w/w) treatments than under CK; however, BG activity in RS did not change (P>0.05) under the PE and PVC treatments compared with the CK treatment (Fig. 3-A). Soil XYL activity was significantly higher in BS than in RS under the treatments with PE5% and PVC5% (w/w). Soil XYL activity in BS was significantly higher under the PVC5% (w/w) treatment but did not change (P>0.05) under the PE or PVC treatments compared with CK (Fig. 3-B). NAG

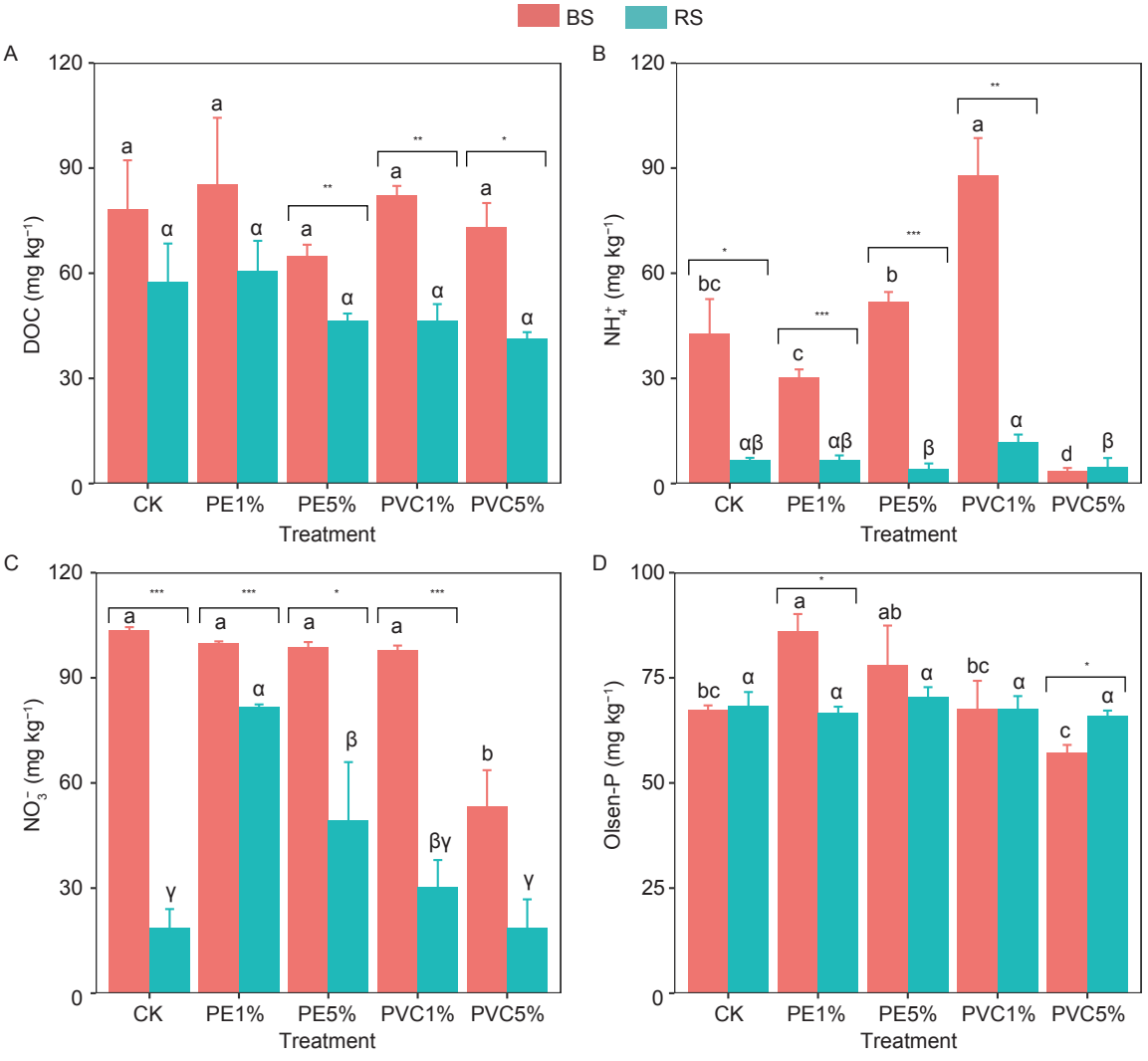


Fig. 2 Dissolved organic carbon (DOC; A), NH_4^+ (B), NO_3^- (C), and Olsen-P (D) concentrations in bulk soil (BS) and rhizosphere soil (RS) at 60 days after planting wheat under five treatments. Treatments include no polyethylene or polyvinyl chloride addition (CK), 1% polyethylene addition (PE1%, w/w), 5% polyethylene addition (PE5%, w/w), 1% polyvinyl chloride addition (PVC1%, w/w), and 5% polyvinyl chloride addition (PVC5%, w/w). Different lowercase letters in Latin and Greek letters indicate significant differences (P<0.05) between RS and BS, respectively. *, **, and *** represent significant differences between RS and BS at P<0.05, P<0.01, and P<0.001, respectively. All results are mean±SE (n=3).

activity was significantly higher in BS than in RS under the treatments with CK, PE5%, and PVC5% (w/w). The NAG activities in BS and RS did not change (P>0.05) under the PE and PVC treatments compared with CK (Fig. 3-C). PHOS showed significantly higher activity in BS than in RS under the treatments with CK, PE5%, and PVC5% (w/w). PHOS activity in BS was significantly lower in the PE (1 and 5%) and PVC1% (w/w) treatments than under CK, and that in RS did not change (P>0.05) in the PE and PVC treatments compared with CK (Fig. 3-D).

3.4. Hotspot and rhizosphere expansion

Compared with CK, the BG hotspots were significantly increased by 278.88 and 123.32% under the PE1% and PVC5% (w/w) treatments, respectively (Fig. 4-A). Compared with CK, the XYL hotspots were significantly increased by 1,198.74 and 1,052.12% under the PVC1% and PVC5% (w/w) treatments, respectively (Fig. 4-B). The NAG hotspot was significantly increased by 3127.23% under the PE1% (w/w) treatment compared with CK (Fig. 4-C). Compared with CK, the PHOS hotspots were significantly reduced by 62.19, 84.35, 95.03, and 84.16% under the PE1%, PE5%, PVC1%, and PVC5% (w/w) treatments, respectively (Fig. 4-D).

For rhizosphere expansion, compared with CK, the level of rhizospheric BG activity was significantly increased by 72.45% under the PVC5% (w/w) treatment (Fig. 4-E). The

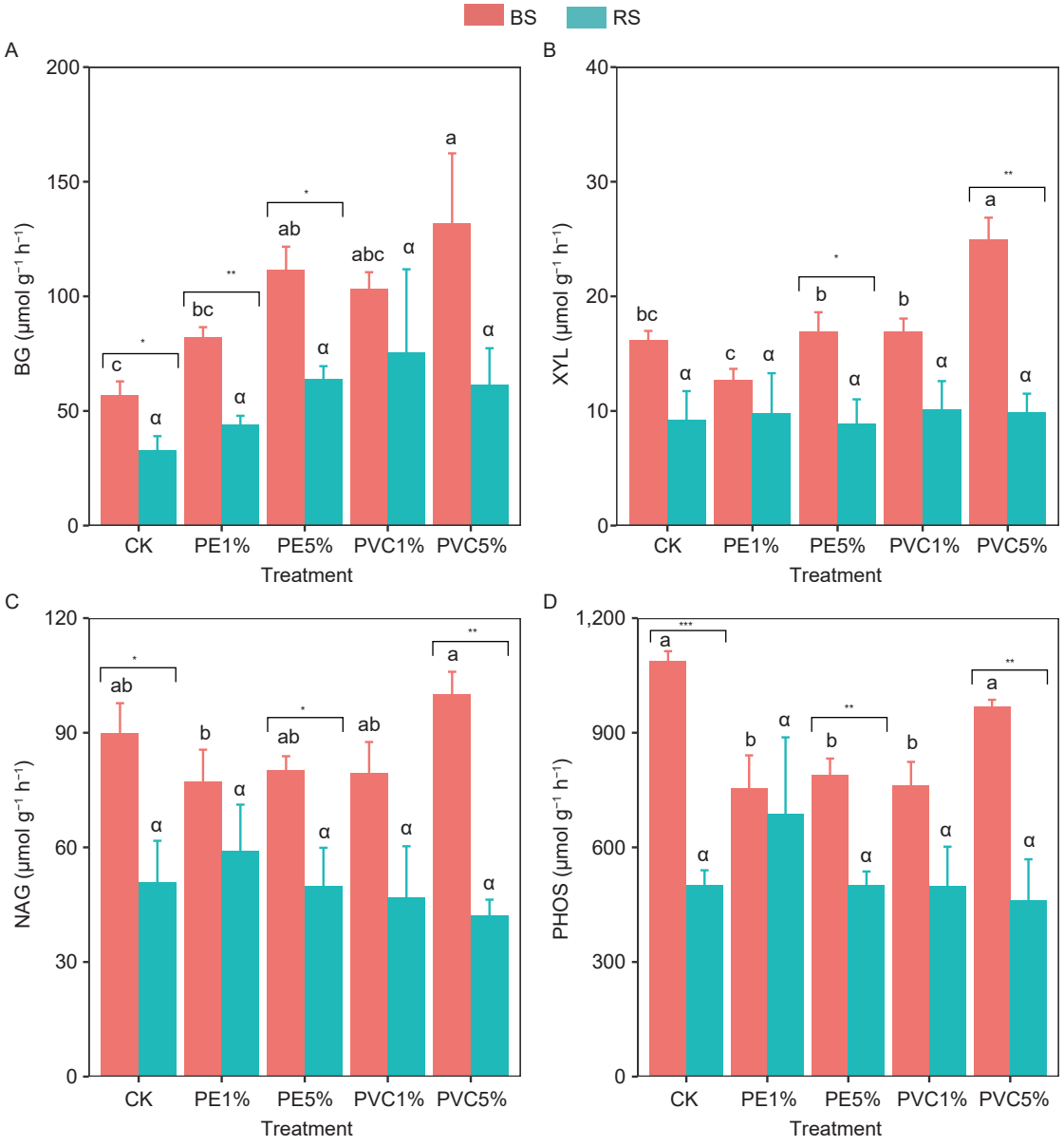


Fig. 3 Potential activities of β-1,4-glucosidase (BG; A), β-1,4-xylosidase (XYL; B), 4-N-acetyl-glucosaminidase (NAG; C), and phosphatase (PHOS; D) in the bulk soil (BS) and rhizosphere soil (RS) at 60 days after planting wheat under five treatments. Treatments include no polyethylene or polyvinyl chloride addition (CK), 1% polyethylene addition (PE1%, w/w), 5% polyethylene addition (PE5%, w/w), 1% polyvinyl chloride addition (PVC1%, w/w), and 5% polyvinyl chloride addition (PVC5%, w/w). Different lowercase letters in Latin and Greek letters indicate significant differences (P<0.05) between RS and BS, respectively. *, **, and *** represent significant differences between RS and BS at P<0.05, P<0.01, and P<0.001, respectively. All results are presented as mean±SE (n=3).

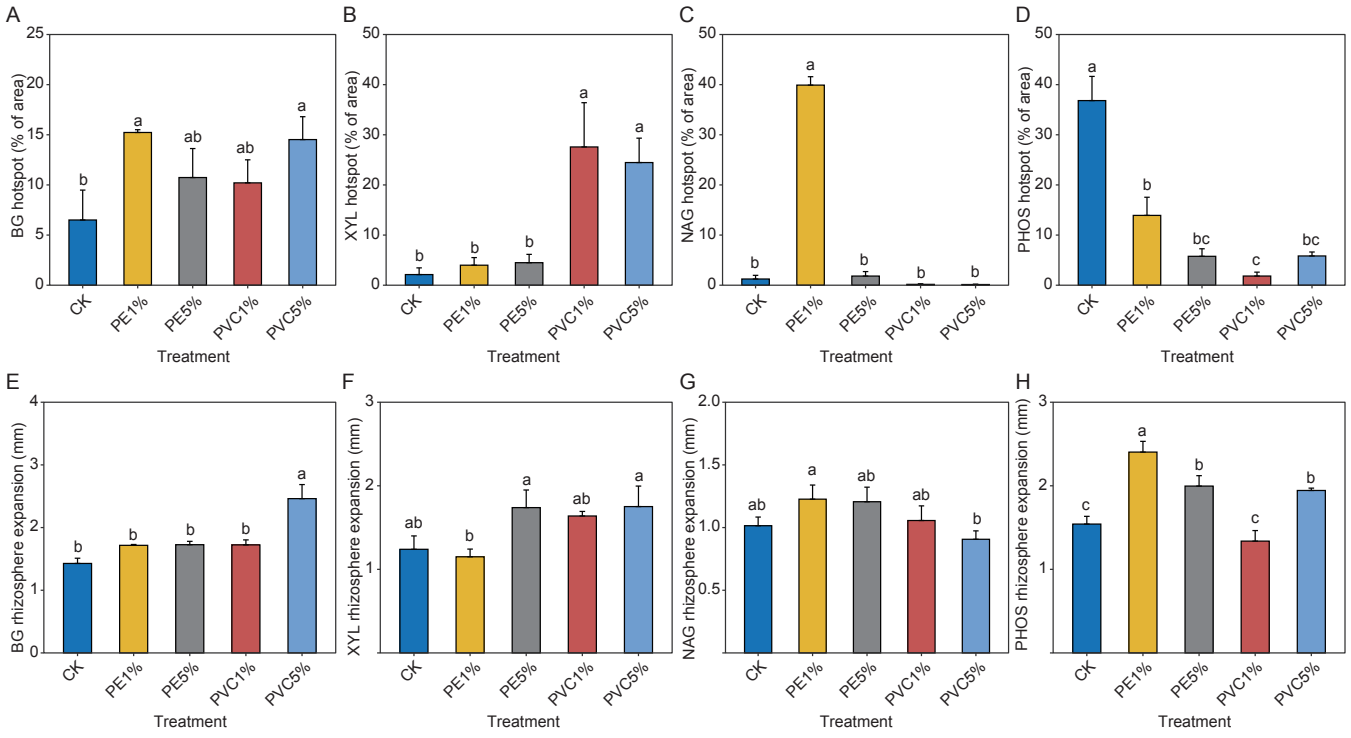


Fig. 4 Enzymatic hotspots and rhizosphere expansion for β-1,4-glucosidase (BG; A), β-1,4-xylosidase (XYL; B), 4-N-acetyl-glucosaminidase (NAG; C), and phosphatase (PHOS; D), and rhizosphere expansion for BG (E), XYL (F), NAG (G), and PHOS (H) at 60 days after planting wheat under five treatments. Treatments include no polyethylene or polyvinyl chloride addition (CK), 1% polyethylene addition (PE1%, w/w), 5% polyethylene addition (PE5%, w/w), 1% polyvinyl chloride addition (PVC1%, w/w), and 5% polyvinyl chloride addition (PVC5%, w/w). All results are presented as mean±SE (*n*=3).

XYL activity did not change (P>0.05) under the PE1%, PE5%, PVC1%, or PVC5% (w/w) treatments compared with CK (Fig. 4-F). Compared with CK, NAG activity did not change (P>0.05) under the PE1%, PE5%, PVC1%, or PVC5% (w/w) treatments (Fig. 4-G). PHOS activity was significantly increased by 55.86, 29.49, and 26.07% under the PE1%, PE5%, and PVC5% (w/w) treatments, respectively, compared with CK (Fig. 4-H).

3.5. Microbial community diversity and co-occurrence network

Regarding the bacterial diversity indices, Chao1 was significantly lower in BS than in RS under the PE1% (w/w) treatment; however, the Chao1 indices in RS did not change (P>0.05) under the PE and PVC treatments compared with CK (Fig. 5-A). Similarly, the Shannon index was significantly lower in BS than in RS under the PE1% (w/w) treatment, while that in the BS was significantly lower in the PE1% (w/w) treatment. This index in the RS was significantly higher under the PE (1 and 5%) (w/w) treatments compared with CK (Fig. 5-B). The Simpson index was significantly lower in BS than in RS under the PE1% (w/w) treatment. The Simpson index in BS was significantly lower compared to CK under the PE1% (w/w) treatment. However, it was significantly higher in RS under the PE and PVC treatments than under CK (Fig. 5-C).

For the fungal diversity indices, Chao1 was significantly lower in BS than in RS under the PVC5% (w/w) treatment. The Chao1 index in BS did not change (P>0.05) under the PE and PVC (1 and 5%) (w/w) treatments, while that in the RS was significantly higher in the PVC5% (w/w) treatment than in CK (Fig. 5-D). Similarly, the Shannon index was significantly lower in BS than in RS under treatment with PVC5% (w/w), while those in BS and RS did not change (P>0.05) under the PE or PVC (1 and 5%) (w/w) treatments compared with CK (Fig. 5-E). The Simpson indices were significantly lower in BS than in RS under treatments with PE5% and PVC5% (w/w). The Simpson index in BS did not change (P>0.05) under the PE and PVC (1 and 5%) (w/w) treatments, while that in the rhizosphere was significantly lower under the PE1% and PVC1% (w/w) treatments than under CK (Fig. 5-F).

According to the LDA, differential bacterial taxa from four and 10 phyla were detected in the BS and RS, respectively, in response to PE and PVC additions (Fig. 6-A). Differential fungal taxa from one and two phyla were detected in the RS and BS, respectively, in response to PE and PVC additions (Fig. 6-B), indicating that wheat root exudates could significantly shift in the presence of bacterial and fungal taxa under treatment with PE and PVC microplastics. Compared with those in the BS, PE and PVC addition reduced the bacterial network complexity but increased that of fungi in the RS due to alterations in the compositions and structures of the bacterial and fungal communities, as well as the decreases or increases in vital network metrics (N or E) (Fig. 6-C and D).

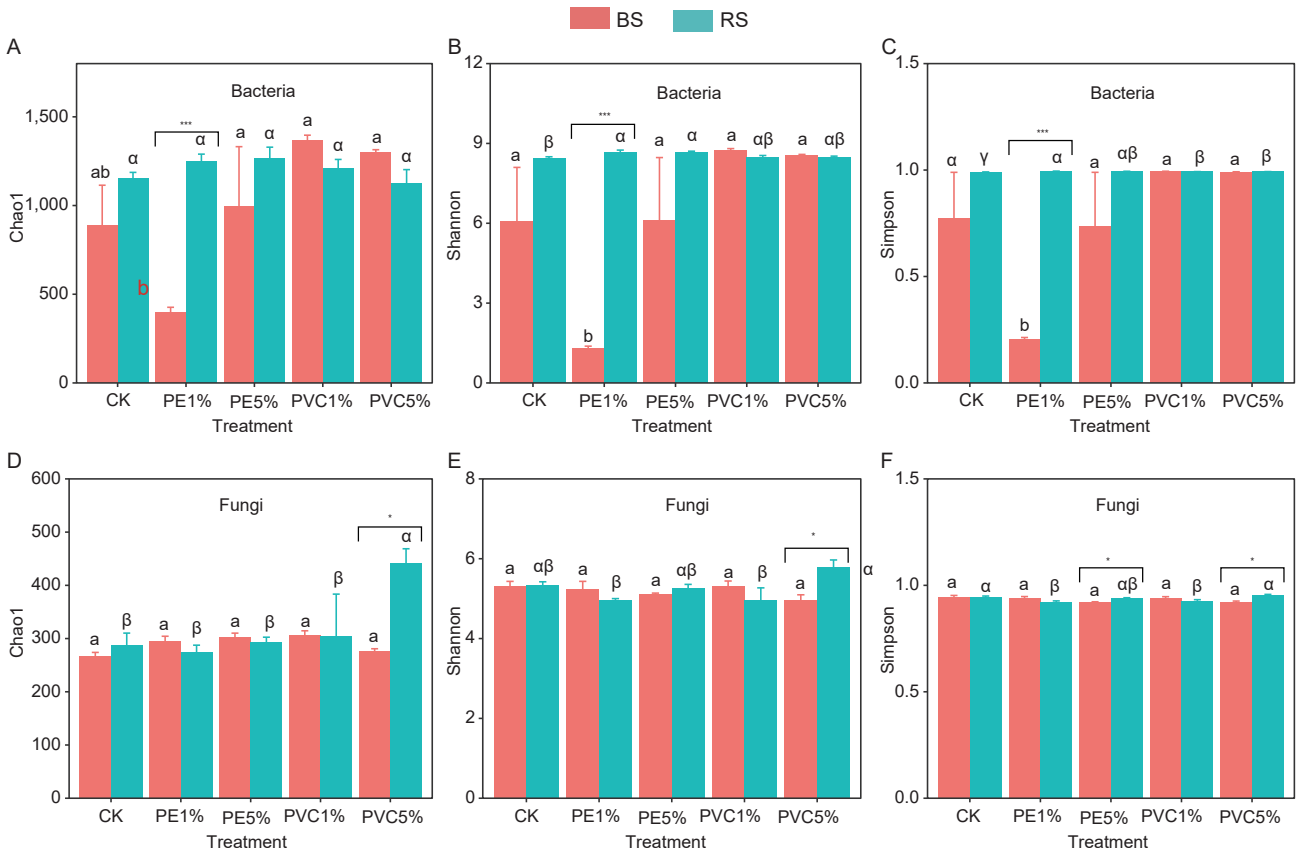


Fig. 5 Chao1 (A), Shannon (B), and Simpson (C) indices of the bacterial diversity, and Chao1 (D), Shannon (E), and Simpson (F) indices of the fungal diversity in bulk soil (BS) and rhizosphere soil (RS) at 60 days after planting wheat under five treatments. Treatments include no polyethylene or polyvinyl chloride addition (CK), 1% polyethylene addition (PE1%, w/w), 5% polyethylene addition (PE5%, w/w), 1% polyvinyl chloride addition (PVC1%, w/w), and 5% polyvinyl chloride addition (PVC5%, w/w). Different lowercase letters in Latin and Greek letters indicate significant differences (P<0.05) between BS and RS, respectively. *, **, and *** represent significant differences between BS and RS at P<0.05, P<0.01, and P<0.001, respectively. All results are presented as mean±SE (n=3).

3.6. Relationships among microbial community diversity, soil available nutrients and hydrolase activity

Mantel tests showed that the Chao1, Shannon, and Simpson indices of the bacterial diversity in BS were significantly positively correlated with Olsen-P. However, the Shannon and Simpson indices of the bacterial diversity in RS had positive correlations with NO_3^- (Fig. 7-A). The Chao1 and Simpson indices of fungal diversity in BS were positively correlated with PHOS activity; however, the Simpson index of fungal diversity in RS was positively correlated with BG activity (Fig. 7-B).

3.7. Effects of microplastics on the rhizospheric microbial community, soil nutrients, soil hydrolase, and NPR

The SEM (Chi-squared=0.898, df=2, P=0.638, GFI=0.979, RMSEA=0.000, SRMR=0.078) indicated that all factors (both biotic and abiotic) accounted for 61% of the NPR variance (Fig. 8). Soil fungal diversity (0.112) and available nutrients (0.038) had positive effects on the NPR. In contrast, wheat enzymatic activity (–0.643), soil bacterial diversity (–0.021), and soil hydrolytic activity (–0.456) had negative effects on NPR (Fig. 8).

4. Discussion

The effects of microplastics on crop–soil systems are complex and multifaceted, and they are strongly related to the type and dose of microplastics (Tong *et al.* 2023; Hu *et al.* 2024). In our results, the co-occurrence networks among bacteria were weakened by microplastics. However, those among fungi were strengthened by the addition of PE and PVC microplastics, with an increase in microbial functionality resilience and enhanced competition with neighboring roots for SOM mining (Song *et al.* 2023). This competition for N and P may adversely affect NPR by reducing SOD activity and increasing POD activity during wheat growth under PE5% and PVC (1% and 5% (w/w)) microplastic treatments. This occurs because the combined stress of antibiotics and PE and PVC microplastics exceeds the defensive capacity of SOD (Li G *et al.* 2023). Contradictory results from the increase in SOD under microplastic addition may indicate that the stress effects vary among cultivars and soil types, highlighting the possibility that the antioxidant defensive system is unstable and differs among various sets of environmental conditions (Li G *et al.* 2023).

Notably, the PE or PVC microplastics at 1 and 5% (w/w) did not change the DOC concentration in either BS or RS; however, at higher doses (5% (w/w)) of PE and PVC

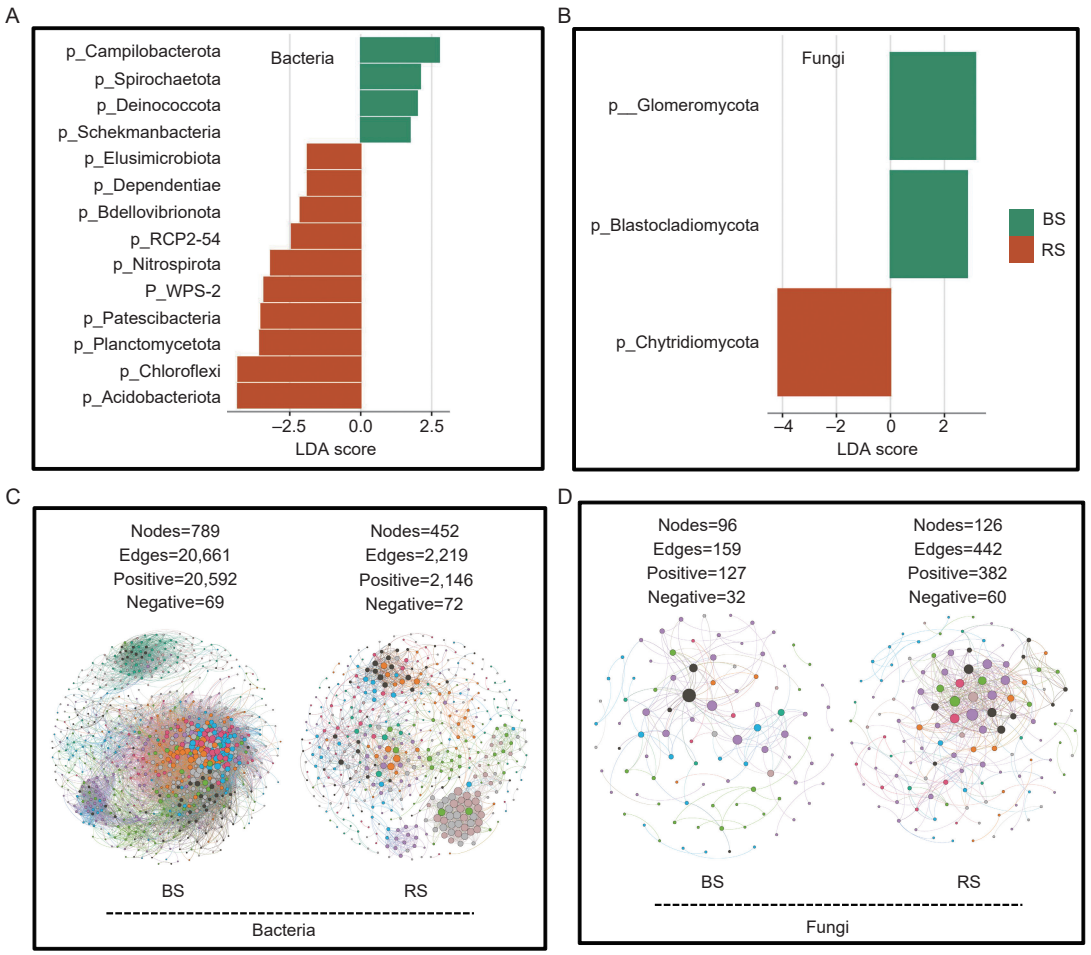


Fig. 6 Differentially abundant taxa in the bacterial (A) and fungal (B) communities, and co-occurrence networks of the bacterial (C) and fungal (D) communities in bulk soil (BS) and rhizosphere soil (RS) at 60 days after planting wheat under five treatments.

microplastics, the DOC concentration in BS was higher than that in RS, indicating that PE and PVC inhibit the production of root exudates by wheat roots due to their toxicity, driving the utilization of labile C by rhizospheric microorganisms (Abbasi *et al.* 2021; Li J *et al.* 2023). Low-molecular-weight organic acids in wheat root exudates have been considered as agents for alleviating microplastic toxicity (Shi R *et al.* 2023). High-dose PE (5% (w/w)) microplastics act as a carrier and transport polycyclic aromatic hydrocarbons from varying sources to the wheat rhizosphere (Abbasi *et al.* 2021). PVC microplastics exert pronounced physicochemical toxicity, which causes the wheat roots to produce less exudates (Wang H *et al.* 2024), resulting in a lower DOC concentration in RS than in BS. Wheat roots are stimulated to expand their growth range and area because of the adverse effects of microplastics in the soil, thereby facilitating symbiotic relationships with mycorrhizal partners to acquire nutrients (Smith and Read 2008; Shi L *et al.* 2023). The C turnover rate of rhizospheric microorganisms was enhanced by the BG hotspots in PE1% and PVC5% (w/w) and the XYL hotspots in PVC (1 and 5%) (w/w); however, inconsistencies were observed in the potential activities of BG and XYL in BS.

Similarly, the microplastic type and dose influence available N and P in the soil (Li *et al.* 2020; Yin *et al.* 2023). Compared with CK, PVC microplastics increased NH_4^+ at 1% (w/w) but not at 5% (w/w); however, PVC1% (w/w) did not change NO_3^- while PVC5% (w/w) reduced NO_3^- without affecting the potential activity of NAG in BS, indicating that PVC5% (w/w) microplastics reduce SOM porosity and hinder oxygen diffusion, causing NO_3^- denitrification (Boots *et al.* 2019; Song *et al.* 2024). PE microplastics increased Olsen-P at 1% but not at 5% (w/w). PVC microplastics at 1 or 5% (w/w) did not change Olsen-P in BS, indicating that microplastic dose strongly affects soil Olsen-P (Liu *et al.* 2023; Wang R *et al.* 2024). In contrast to our results, Shi L *et al.* (2023) found that PE5% (w/w) microplastics significantly reduced the Olsen-P concentration. Wang R *et al.* (2024) also showed that PE and PVC microplastics substantially reduced soil Olsen-P by 9.7–38.6%, and that a high concentration (5% (w/w)) of microplastics caused pronounced reductions in Olsen-P. Based on these inconsistencies, we infer that the soil type caused this difference (Shi *et al.* 2022).

Microplastics alter the soil biotic and abiotic environments, thereby affecting crop nutrient availability (Iqbal *et al.* 2023). Compared with CK, the NO_3^- concentration was increased by PE microplastics (1 and 5% (w/w)), along with an increase in NAG hotspots at 1% (w/w) PE microplastics in RS. This occurs because wheat roots release root exudates, including

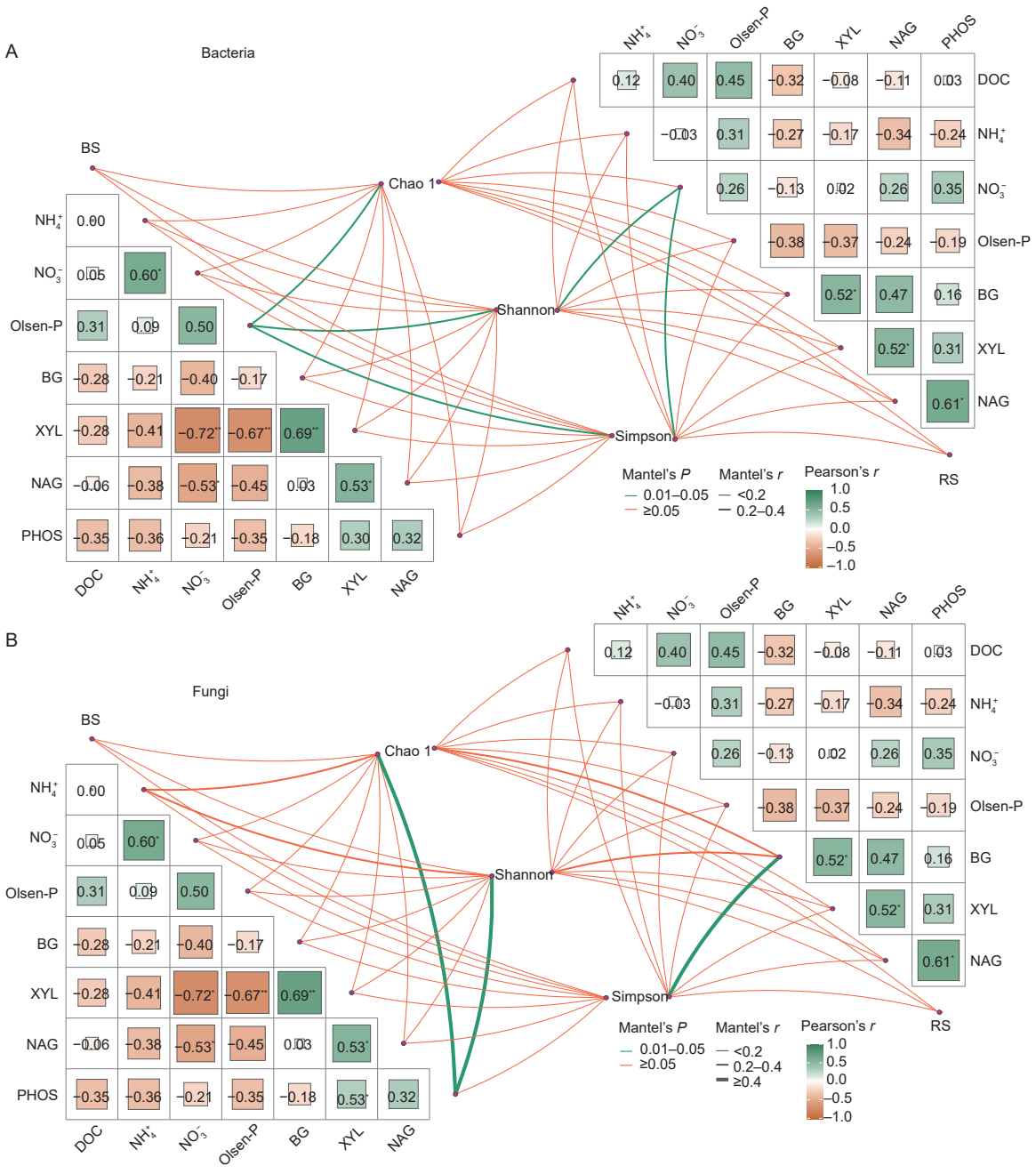


Fig. 7 Factors regulating the correlations between soil available nutrients and hydrolase activity with microbial community diversity as measured by the Chao1, Shannon, and Simpson indices of bacterial diversity (A) as well as the Chao1, Shannon, and Simpson indices of fungi diversity (B) in bulk soil (BS) and rhizosphere soil (RS), as revealed by the Mantel test upon PE and PVC addition. BG, β-1,4-glucosidase; XYL, β-1,4-xylosidase; NAG, 4-N-acetyl-glucosaminidase; PHOS, phosphatase; DOC, dissolved organic C. Pairwise correlations among soil available nutrients and hydrolase activity are also presented (*, P<0.05 ; **, P<0.01).

organic acids and NO_3^-, resulting in increased aromaticity and hydrophobic components (Cai *et al.* 2024). However, PE microplastics inhibit organic acids in root exudates to mine SOM using rhizospheric microorganisms to acquire available N during wheat growth (Liu Y *et al.* 2022). The Olsen-P concentration did not change with decreasing PHOS hotspots, however increasing PHOS rhizosphere expansion under PE and PVC microplastic (1 or 5% (w/w)) treatments, indicating that wheat roots need to acquire available P through the survival strategy of relatively broad root growth under microplastic addition (Sahasa *et al.* 2023). In our results, the potential activities of BG and XYL in BS were increased, whereas that of PHOS was reduced under the PVC5%, PE (1 and 5%) (w/w), and PVC1% (w/w) treatments, demonstrating that microplastics cause oxidative damage to the crops and disrupt metabolic activities (Iqbal *et al.* 2023). Nevertheless, the levels of BG, XYL, NAG, and PHOS in RS did not change, possibly because the microplastics were either adsorbed onto the crop root surface or accumulated in their vascular systems, consequently inhibiting nutrient

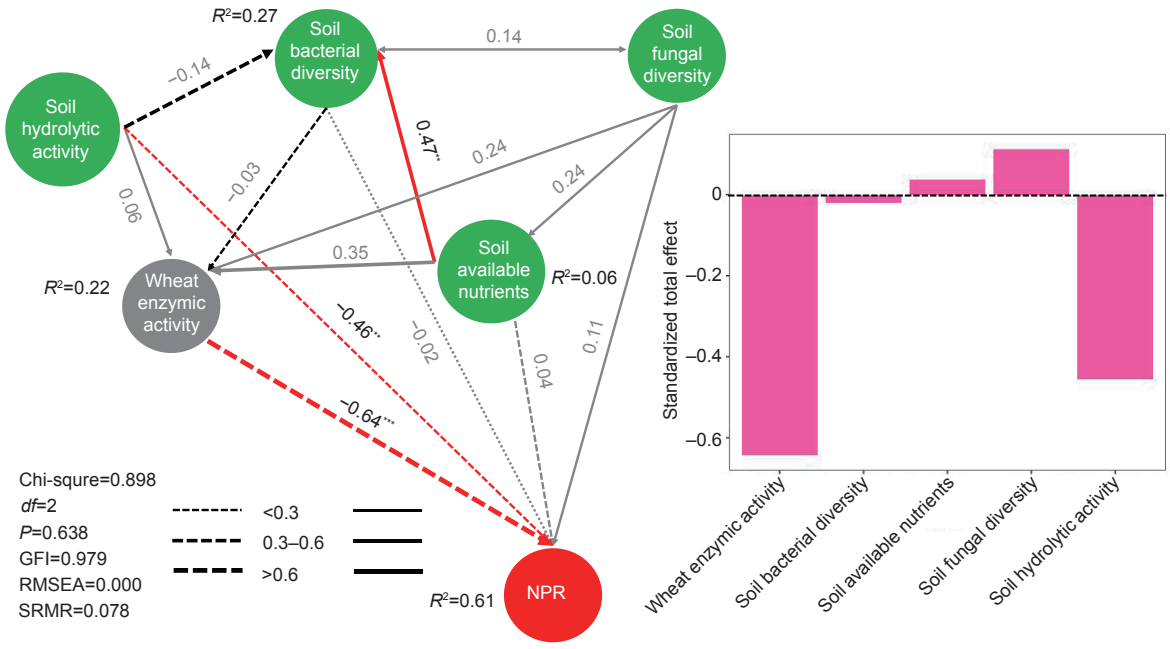


Fig. 8 Structural equation model (SEM) of the effects of microplastic addition on the net photosynthetic rate (NPR) and standardized total effects of soil fungal diversity, soil available nutrients, wheat enzymatic activities, and soil bacterial diversity on the NPR of wheat rate. Arrow widths indicate the strength of the standardized path coefficients. Solid lines indicate positive path coefficients and dashed lines indicate negative path coefficients. R^2 values indicate the proportion of variance explained by each variable contributing to NPR from wheat rhizosphere soil amended with polyethylene (PE) and polyvinyl chloride (PVC) microplastics. **, P<0.01; ***, P<0.001.

acquisition (Iqbal *et al.* 2023).

Microplastics affect the diversity of microbial communities (Yin *et al.* 2023; Hu *et al.* 2024). The Chao1, Shannon, and Simpson indices of bacterial diversity declined in PE-amended BS (1% (w/w)), possibly because PE particles act as C inputs that inhibit the bacterial population (Song *et al.* 2023); however, this adverse effect was absent at a high PE dose (5% (w/w)). The Shannon and Simpson indices of bacterial diversity increased in the PE- and PVC-amended RS, indicating that labile C from wheat root exudates weakens the adverse effects of PE or PVC, favoring the growth of rhizospheric bacterial communities (Liu *et al.* 2021). Thus, the p_Elusimicrobiota, p_Dependentiae, p_Bdellovibrionota, p_RCP2-54, p_Nitrospirota, p_WPS-2, p_Patescibacteria, p_Chloroflexi, and p_ Acidobacteria bacterial taxa were dominant in RS, which is consistent with a study which showed that the degree to which the plastisphere and soil bacterial communities differed was negatively correlated with soil pH and carbon content (Sun *et al.* 2024). Microplastics have a strong capacity for absorbing labile C and inorganic P (Olsen-P) (Li *et al.* 2022), resulting in the positive Shannon and Simpson indices of bacterial diversity in the BS for Olsen-P. However, the Shannon and Simpson indices of bacterial diversity in the RS were positive for NO_3^-, implying that N can be obtained through N uptake by roots during wheat growth under microplastic stress, which could block the wheat nutrient transport pathways (Geng *et al.* 2024; Yang *et al.* 2024).

The Chao1 of fungal diversity did not change under PE treatments in either the BS or RS, but it increased in the PVC-amended RS (5% (w/w)). However, the Chao1, Shannon, and Simpson indices of fungal diversity in the PVC-amended RS (5% (w/w)) were higher than in the PVC-amended BS (5% (w/w)), possibly because a high-dose of PVC (5% (w/w)) particles increases the rhizospheric fungal communities (Hu *et al.* 2024). In BS, p_Glomeromycota and p_Blastoctadiomycota were dominant, while only p_Chytridiomycota existed in RS, indicating that labile C from wheat root exudates could also change the fungal taxa in the soil due to changes in microbial nutrient acquisition strategies during wheat growth. The fungal community on the surface of microplastics catalyzes metabolic reactions to promote microplastic and SOM decomposition for enhancing wheat growth (Fan *et al.* 2022; Liu Y *et al.* 2022). The Chao1 and Simpson indices of fungal diversity in the BS positively affected PHOS activity due to the strong adsorption capacity of microplastics for Olsen-P (P-limited) (Li *et al.* 2022). However, the Simpson index of fungal diversity in the RS had a positive effect on BG activity, demonstrating that microplastics absorb labile C from wheat root exudates (Li *et al.* 2022), which limits the C available to increase fungal growth in the RS under microplastic stress.

Under different stresses (microplastic types and doses), plants constantly regulate their antioxidant enzyme activities to rigorously manage reactive oxygen species levels (Li G *et al.* 2023). POD activity increased in response to PE and PVC microplastic addition, indicating that POD is crucial for regulating oxidative stress to protect plant tissues. It acts as a vital reactive oxygen species scavenger and defense mechanism in wheat by reducing the diversity of microbial communities under PE (1%) and PVC (1 and 5% (w/w)) microplastic addition, consistent with the findings of Guo *et al.* (2022). In this process, the wheat root system faces

the stress of microplastics by increasing root growth for the autochthonous uptake of more nutrients; however, the wheat root can only take up limited amounts of nutrients that are available before the microplastics become attached to the root system or are absorbed into the roots, resulting in lower nutrient levels in RS than in BS (Yang *et al.* 2024). Wheat roots secrete root secretions, thereby reducing extracellular enzyme production in RS and regulating the ranges and sizes of hydrolase hotspots and rhizosphere expansion (Liu Y *et al.* 2022). Therefore, wheat has a strong antioxidant defense strategy in response to PE and PVC microplastic stress, which produces a synergistic effect of POD in protecting organelles and reducing tissue damage (Ahammed *et al.* 2012; Jeyavani *et al.* 2023). Finally, the reduction in NPR occurred due to changes in the antioxidant defense system caused by microplastic accumulation.

5. Conclusion

The type and dose of PE and PVC microplastics affected the NPR through an antioxidant defense strategy *via* two pathways. In RS, the Chao1, Shannon, and Simpson indices of the bacterial and fungal diversities positively affected NO_3^- and BG, indicating that NO_3^- and C resources are the limiting factors for microorganisms. However, the potential hydrolase activities in RS were inconsistent with the hydrolase hotspots and rhizosphere expansion with an extended root system. Therefore, wheat has a strong antioxidant defense strategy, producing a synergistic effect of POD in protecting organelles and reducing tissue damage, even with two wheat nutrient acquisition strategies operating in response to PE and PVC microplastic stress. Finally, the reduction in NPR occurred through rhizospheric effects due to changes in the activities of antioxidant enzymes and the synthesis of antioxidant substances caused by microplastic accumulation.

Acknowledgements

This research was supported by the National Natural Science Foundation of China (42407458 and 42307420), the Global Challenges Research Fund of the UK Natural Environment Research Council (NE/V005871/1) and the Shandong Province First-class Discipline Construction “811” Project, China.

Declaration of competing interest

The authors declare that they have no conflict of interest.

Declaration of generative AI and AI-assisted technologies in scientific writing process

The authors declare that they did not use AI in the preparation and writing of this manuscript.

References

Abbasi S, Moore F, Keshavarzi B. 2021. PET-microplastics as a vector for polycyclic aromatic hydrocarbons in a simulated plant rhizosphere zone. *Environmental Technology and Innovation*, **21**, 101370.

Aggarwal S L, Sweeting O J. 1957. Polyethylene: Preparation, structure, and properties. *Chemical Reviews*, **57**, 665–672.

Ahammed G J, Wang M M, Zhou Y H, Xia X J, Mao W H, Shi K, Yu J Q. 2012. The growth, photosynthesis and antioxidant defense responses of five vegetable crops to phenanthrene stress. *Ecotoxicology and Environmental Safety*, **80**, 132–139.

Bilyera N, Kuzyakova I, Guber A, Razavi B S, Kuzyakov Y. 2020. How “hot” are hotspots: Statistically localizing the high-activity areas on soil and rhizosphere images. *Rhizosphere*, **16**, 100259.

Boots B, Russell C W, Green D S. 2019. Effects of microplastics in soil ecosystems: Above and below ground. *Environmental Science and Technology*, **53**, 11059–11614.

Brodhagen M, Goldberger J R, Hayes D G, Inglis D A, Marsh T L, Miles C. 2017. Policy considerations for limiting unintended residual plastic in agricultural soils. *Environmental Science and Policy*, **69**, 81–84.

Cai Y, Xu Y, Liu G, Li B, Guo T, Ouyang D, Li M, Liu S, Tan Y, Wu X, Zhang H. 2024. Polyethylene microplastic modulates lettuce root exudates and induces oxidative damage under prolonged hydroponic exposure. *Science of the Total Environment*, **916**, 170253.

Caporaso J G, Kuczynski J, Stombaugh J, Bittinger K, Bushman F D, Costello E K, Fierer N, Pẽa A G, Goodrich J K, Gordon J I, Huttley G A, Kelley S T, Knights D, Koenig J E, Ley R E, Lozupone C A, McDonald D, Muegge B D, Pirrung M, Reeder J, *et al*. 2010. QIIME allows analysis of high-throughput community sequencing data. *Nature Methods*, **7**, 335–341.

Fan P, Tan W, Yu H. 2022. Effects of different concentrations and types of microplastics on bacteria and fungi in alkaline soil. *Ecotoxicology and Environmental Safety*, **229**, 113045.

Ganesh Kumar A K, Anjana K, Hinduja M, Sujitha K, Dharani G. 2020. Review on plastic wastes in marine environment-Biodegradation and biotechnological solutions. *Marine Pollution Bulletin*, **150**, 110733.

Geng S, Li L, Miao Y, Zhang Y, Yu X, Zhang D, Yang Q, Zhang X, Wang Y. 2024. Nitrogen rhizodeposition from corn and soybean, and its contribution to the subsequent wheat crops. *Journal of Integrative Agriculture*, **23**, 2446–2457.

Guo A, Pan C, Su X, Zhou X, Bao Y. 2022. Combined effects of oxytetracycline and microplastic on wheat seedling growth and associated rhizosphere bacterial communities and soil metabolite profiles. *Environmental Pollution*, **302**, 119046.

Hu Z, Xiao M, Wu J, Tong Y, Ji J, Huang Q, Ding F, Ding J, Zhu Z, Chen J, Ge T. 2024. Effects of microplastics on photosynthesized C allocation in a rice–soil system and its utilization by soil microbial groups. *Journal of Hazardous Materials*, **466**, 133540.

Iqbal B, Zhao T, Yin W, Zhao X, Xie Q, Khan K Y, Zhao X, Nazar M, Li G, Du D. 2023. Impacts of soil microplastics on crops: A review. *Applied Soil Ecology*, **181**, 104680.

Jebara S, Jebara M, Limam F, Aouani M E. 2005. Changes in ascorbate peroxidase, catalase, guaiacol peroxidase and superoxide dismutase activities in common bean (*Phaseolus vulgaris*) nodules under salt stress. *Journal of Plant Physiology*, **162**, 929–936.

Jeyavani J, Sibiya A, Gopi N, Mahboob S, Al-Ghanim K A, Al-Misned F, Ahmed Z, Riaz M N, Palaniappan B, Govindarajan M, Vaseeharan B. 2023. Ingestion and impacts of water-borne polypropylene microplastics on daphnia similis. *Environmental Science and Pollution Research*, **30**, 13483–13494.

Khan, K Y, Ali B, Zhang S, Stoffella P J, Yuan S, Xia Q, Qu H, Shi Y, Cui X, Guo Y. 2021. Effects of antibiotics stress on growth variables, ultrastructure, and metabolite pattern of *Brassica rapa* ssp. chinensis. *Science of the Total Environment*, **778**, 146333.

Li C, Cui Q, Li Y, Zhang K, Lu X, Zhang Y. 2022. Effect of LDPE and biodegradable PBAT primary microplastics on bacterial community after four months of soil incubation. *Journal of Hazardous Materials*, **429**, 128353.

Li G, Tang Y, Khan K Y, Son Y, Jung J, Qiu X, Zhao X, Iqbal B, Stoffella P J, Kim G J, Du D. 2023. The toxicological effect on pak choi of co-exposure to degradable and non-degradable microplastics with oxytetracycline in the soil. *Ecotoxicology and Environmental Safety*, **268**, 115707.

Li J, Yu Y, Chen X, Yu S, Cui M, Wang S, Song F. 2023. Effects of biochar on the phytotoxicity of polyvinyl chloride microplastics. *Plant Physiology and Biochemistry*, **195**, 228–237.

Li L, Song K, Yeerken S, Geng S, Liu D, Dai Z, Xie F, Zhou X, Wang Q. 2020. Effect evaluation of microplastics on activated sludge nitrification and denitrification. *Science of the Total Environment*, **707**, 135953.

Liu S, Huang K, Yuan G, Yang C. 2022. Effects of polyethylene microplastics and phenanthrene on soil properties, enzyme activities and bacterial communities. *Processes*, **10**, 102128.

Liu S L, Jian M F, Zou L, Hu Q W. 2022. Microbial community structure on microplastic surface in the grus leucogeranus reserve of Poyang Lake. *Huanjing Kexue/Environmental Science*, **43**, 1447–1454. (in Chinese)

Liu Y, Shahbaz M, Fang Y, Li B, Wei X, Zhu Z, Mar Lynn T, Lu S, Shibistova O, Wu J, Guggenberger G, Ge T. 2021. Stoichiometric theory shapes enzyme kinetics in paddy bulk soil but not in rhizosphere soil. *Land Degradation and Development*, **33**, 246–256.

Liu Y, Shahbaz M, Ge T, Zhu Z, Liu S, Chen L, Wu X, Deng Y, Lu S, Wu J. 2020. Effects of root exudate stoichiometry on CO_2 emission from paddy soil. *European Journal of Soil Biology*, **101**, 103247.

Liu Y, Xiao M, Shahbaz M, Hu Z, Zhu Z, Lu S, Yu Y, Yao H, Chen J, Ge T. 2022. Microplastics in soil can increase nutrient uptake by wheat. *Journal of Hazardous Materials*, **438**, 129547.

Liu Y, Zhong Y, Hu C, Xiao M, Ding F, Yu Y, Yao H, Zhu Z, Chen J, Ge T, Ding J. 2023. Distribution of microplastics in soil aggregates after film mulching. *Soil Ecology Letters*, **5**, 2662–2289.

Liu Z, Wen J, Liu Z, Wei H, Zhang J. 2024. Polyethylene microplastics alter soil microbial community assembly and ecosystem multifunctionality. *Environment International*, **183**, 108360.

Lozano Y M, Aguilar-Trigueros C A, Onandia G, Maaß S, Zhao T, Rillig M C. 2021. Effects of microplastics and drought on soil ecosystem functions and multifunctionality. *Journal of Applied Ecology*, **58**, 988–996.

Ma X, Shan J, Chai Y, Wei Z, Li C, Jin K, Zhou H, Yan X, Ji R. 2024. Microplastics enhance nitrogen loss from a black paddy soil by shifting nitrate reduction from DNRA to denitrification and anammox. *Science of the Total Environment*, **906**, 167869.

Ng E L, Huerta Lwanga E, Eldridge S M, Johnston P, Hu H W, Geissen V, Chen D. 2018. An overview of microplastic and nanoplastic pollution in agroecosystems. *Science of the Total Environment*, **627**, 1377–1388.

Olsen S R, Cole C V, Watandbe F, Dean L. 1954. *Estimation of Available Phosphorus in Soil by Extraction with Sodium Bicarbonate*. U.S. Department of Agriculture, Circular 939.

Ren X, Tang J, Wang L, Liu, Q. 2021. Microplastics in soil–plant system: Effects of nano/microplastics on plant photosynthesis, rhizosphere microbes and soil properties in soil with different residues. *Plant and Soil*, **462**, 561–576.

Sahasa R G K, Dhevagi P, Poornima R, Ramya A, Moorthy P S, Alagirisamy B, Karthikeyan S. 2023. Effect of polyethylene microplastics on seed germination of Blackgram (*Vigna mungo* L.) and Tomato (*Solanum lycopersicum* L.). *Environmental Advances*, **11**, 100349.

Shi J, Wang J, Lv J, Wang Z, Peng Y, Shang J, Wang X. 2022. Microplastic additions alter soil organic matter stability and bacterial community under varying temperature in two contrasting soils. *Science of the Total Environment*, **838**, 156471.

Shi L, Chen, Z, Hou Y, Li J, Shen Z, Chen Y. 2023. The original polyethylene microplastics inhibit the growth of sweet potatoes and increase the safety risk of cadmium. *Frontiers in Plant Science*, **14**, 1138281.

Shi R, Liu W, Lian Y, Zeb A, Wang Q. 2023. Type-dependent effects of microplastics on tomato (*Lycopersicon esculentum* L.): Focus on root exudates and metabolic reprogramming. *Science of the Total Environment*, **859**, 160025.

Smith S E, Read D J. 2008. *Mycorrhizal Symbiosis*. 3rd ed. Academic Press, San Diego.

Song B, Shang S, Cai F M, Liu Z, Fang J, Li N, Adams J M, Razavi B S. 2023. Microbial resistance in rhizosphere hotspots under biodegradable and conventional microplastic amendment: Community and functional sensitivity. *Soil Biology and Biochemistry*, **180**, 108989.

Song Q, Zhang J, Zhang F, Shen Y, Yue S, Li S. 2024. Optimized nitrogen application for maximizing yield and minimizing nitrogen loss in film mulching spring maize production on the Loess Plateau, China. *Journal of Integrative Agriculture*, **23**, 1671–1684

de Souza Machado A A, Kloas W, Zarfl C, Hempel S, Rillig M C. 2018. Microplastics as an emerging threat to terrestrial ecosystems. *Global Change Biology*, **24**, 1405–1416.

Sun Y, Duan C, Cao N, Li X, Li X, Chen Y, Huang Y, Wang J. 2022. Effects of microplastics on soil microbiome: The impacts of polymer type, shape, and concentration. *Science of the Total Environment*, **806**, 150516.

Sun Y, Wu M, Xie S, Zang J, Wang X, Yang Y, Li C, Wang J. 2024. Homogenization of bacterial plastisphere community in soil: A continental-scale microcosm study. *ISME Communications*, **4**, ycad012.

De Tender C, Devriese L I, Haegeman A, Maes S, Vangeyte J, Cattrijsse A, Dawyndt P, Ruttink T. 2017. Temporal dynamics of bacterial and fungal colonization on plastic debris in the north sea. *Environmental Science and Technology*, **51**, 7350–7360.

Terefe N S, Yang Y H, Knoerzer K, Buckow R, Versteeg C. 2010. High pressure and thermal inactivation kinetics of polyphenol oxidase and peroxidase in strawberry puree. *Innovative Food Science and Emerging Technologies*, **11**, 52–60.

Tong Y, Ding J, Xiao M, Shahbaz M, Zhu Z, Chen M, Kuzyakov Y, Deng Y, Chen J, Ge T. 2023. Microplastics affect activity and spatial distribution of C, N, and P hydrolases in rice rhizosphere. *Soil Ecology Letters*, **5**, 220138.

Wang H, He Y, Zheng Q, Yang Q, Wang J, Zhu J, Zhan X 2024. Toxicity of photoaged polyvinyl chloride microplastics to wheat seedling roots. *Journal of Hazardous Materials*, **463**, 132816.

Wang R, Yang L, Guo M, Lin X, Wang R, Guo S. 2024. Effects of microplastic properties and dissolved organic matter on phosphorus availability in soil and aqueous mediums. *Environmental Pollution*, **340**, 122784.

Wei X, Razavi B, Hu Y, Xu X, Zhu Z, Liu Y, Kuzyakov Y, Li Y, Wu J, Ge T. 2019. C/P stoichiometry of dying rice root defines the spatial distribution and dynamics of enzyme activities in root-detritusphere. *Biology and Fertility of Soils*, **55**, 251–263.

Wei X, Zhu Z, Liu Y, Luo Y, Deng Y, Xu X, Liu S, Richter A, Shibistova O, Guggenberger G, Wu J, Ge T. 2020. C:N:P stoichiometry regulates soil organic carbon mineralization and concomitant shifts in microbial community composition in paddy soil. *Biology and Fertility of Soils*, **56**, 1093–1107.

Winkler D E. 1959. Mechanism of polyvinyl chloride degradation and stabilization. *Journal of Polymer Science*, **35**, 3–6.

Xiao M, Ding J, Luo Y, Zhang H, Yu Y, Yao H, Zhu Z, Chadwick D R, Jones D, Chen J, Ge T. 2022. Microplastics shape microbial communities affecting soil organic matter decomposition in paddy soil. *Journal of Hazardous Materials*, **431**, 128589.

Yang L, Shen P, Liang H, Wu Q. 2024. Biochar relieves the toxic effects of microplastics on the root-rhizosphere soil system by altering root expression profiles and microbial diversity and functions. *Ecotoxicology and Environmental Safety*, **271**, 115935.

Yin M, Yan B, Wang H, Wu Y, Wang X, Wang J, Zhu Z, Yan X, Liu Y, Liu M, Fu C. 2023. Effects of microplastics on nitrogen and phosphorus cycles and microbial communities in sediments. *Environmental Pollution*, **318**, 120852.

Yuan Y, Zhao W, Xiao J, Zhang Z, Qiao M, Liu Q, Yin H. 2017. Exudate components exert different influences on microbially mediated C losses in simulated rhizosphere soils of a spruce plantation. *Plant and Soil*, **419**, 127–140.

Zang H, Zhou J, Marshall M R, Chadwick D R, Wen Y, Jones D L. 2020. Microplastics in the agroecosystem: Are they an emerging threat to the plant-soil system? *Soil Biology and Biochemistry*, **148**, 107926.

Zhang Q F, Li Y Y. 2005. NaCl enhances thylakoid-bound SOD activity in the leaves of C_3 halophyte *Suaeda salsa* L. *Plant Science*, **168**, 423–430.

Zhang K, Wang M, Li Y, Zhang X, Xiao K, Ma C, Zhang X, Zhang H, Chen Y. 2024. Wheat (*Triticum aestivum* L.) seedlings performance mainly affected by soil nitrate nitrogen under the stress of polyvinyl chloride microplastics. *Scientific Reports*, **14**, 4962.

Zhang S, Gao W, Cai K, Liu T, Wang X. 2022. Effects of microplastics on growth and physiological characteristics of tobacco (*Nicotiana tabacum* L.). *Agronomy*, **12**, 2692.

Zhou J, Wen Y, Marshall M R, Zhao J, Gui H, Yang Y, Zeng Z, Jones D L, Zang H. 2021. Microplastics as an emerging threat to plant and soil health in agroecosystems. *Science of the Total Environment*, **787**, 147444.

Executive Editor-in-Chief Jinshui Wu
Managing Editor Lujuan Sun